

Supplemental Materials for:

CD163+ Macrophages Promote Angiogenesis, Vascular Permeability, and Inflammation in Atherosclerosis

Liang Guo^{1*}, Hirokuni Akahori^{2,a*}, Emanuel Harari^{1,b*}, Samantha L. Smith¹, Rohini Polavarapu², Vinit Karmali², Fumiya Otsuka^{1,c}, Rachel L. Gannon¹, Ryan E. Braumann¹, Megan H. Dickinson¹, Anuj Gupta³, Audrey L. Jenkins⁴, Michael J. Lipinski⁴, Johoon Kim⁵, Peter Chhour⁵, Paul S. de Vries⁶, Hiroyuki Jinnouchi¹, Robert Kutys¹, Hiroyoshi Mori¹, Matthew D. Kutyna¹, Sho Torii¹, Atsushi Sakamoto¹, Cheol Ung Choi^{2,d}, Qi Cheng¹, Megan L. Grove⁶, Mariem A. Sawan³, Yin Zhang⁷, Yihai Cao⁷, Frank D. Kolodgie¹, David P. Cormode⁵, Dan E. Arking⁸, Eric Boerwinkle^{6,9}, Alanna C. Morrison⁶, Jeanette Erdmann¹⁰, Nona Sotoodehnia¹¹, Renu Virmani¹ and Alope V. Finn^{1,3†}

1. CVPPath Institute, Gaithersburg, Maryland, USA.
 2. Department of Medicine, Emory University School of Medicine, Atlanta, Georgia, USA.
 3. Department of Medicine, University of Maryland School of Medicine, Baltimore, Maryland, USA.
 4. Medstar Health Research Institute, MedStar Washington Hospital Center, Washington, DC, USA.
 5. Department of Radiology, Perelman School of Medicine, University of Pennsylvania, Philadelphia, Pennsylvania, USA.
 6. Human Genetics Center, Department of Epidemiology, Human Genetics, and Environmental Sciences, School of Public Health, The University of Texas Health Science Center at Houston, Houston, Texas, USA
 7. Department of Microbiology, Tumor and Cell Biology, Karolinska Institute, 171 77 Stockholm, Sweden.
 8. McKusick-Nathans Institute of Genetic Medicine, Johns Hopkins University School of Medicine, Baltimore, Maryland, USA.
 9. Human Genome Sequencing Center, Baylor College of Medicine, Houston, Texas, USA
 10. Institute for Cardiogenetics, University of Lübeck, and German Centre for Cardiovascular Research (DZHK), Partner Site Hamburg/Kiel/Lübeck, Germany.
 11. Division of Cardiology, Department of Medicine and Epidemiology, Cardiovascular Health Research Unit, University of Washington, Seattle, Washington, USA.
-
- a. Current address: Department of Internal Medicine, Cardiovascular Division, Hyogo College of Medicine, Nishinomiya, Hyogo, Japan
 - b. Current address: Division of Cardiology, Rabin Medical Center, Petah-Tikva, and Sackler Faculty of Medicine, Tel-Aviv University, Tel Aviv, Israel
 - c. Current address: National Cerebral and Cardiovascular Center, Suita, Osaka, Japan
 - d. Current address: Cardiovascular Center, Division of Cardiology, Departments of Internal Medicine, Korea University Guro Hospital, Guro-gu, Seoul, Korea.

*These authors contributed equally to this work.

†To whom correspondence should be addressed:

Aloke V. Finn, M.D.

CVPath Institute

19 Firstfield Road

Gaithersburg, Maryland, 20878

University of Maryland School of Medicine

Baltimore, Maryland, 21201

Phone: 301-208-3570

Fax: 301-208-3745

Email: afinn@cvpath.org

Supplemental Methods

Cell culture. Human monocytes were collected from healthy volunteers (Astarte Biologics, Redmond, WA) were differentiated over 7-days into macrophages in RPMI 1640 medium (Gibco, Invitrogen) supplemented with 10% human serum (Invitrogen). Prior to use, hemoglobin (lyophilized stabilized purified A₀ ferrous hemoglobin (Sigma Aldrich)) and haptoglobin phenotype 1-1 (lyophilized purified (Sigma Aldrich)) were reconstituted in sterile phosphate buffered solution (PBS) at a concentration of 0.1 mg/ml. Equimolar amounts of hemoglobin and haptoglobin in growth medium were used to generate hemoglobin:haptoglobin complexes (HH), which were added to cultured monocytes at 4 hours after plating. We differentiated human monocytes over 7-days in HH complexes which reproduced the phenotype seen in human atherosclerotic plaques at areas of hemorrhage as previously described (1). For hepcidin experiments, differentiated human macrophages were washed and exposed to control media or human hepcidin (Hepcidin, 700 nmol/L for 24 hours, Anaspec) on day 6 prior to harvest on day 7. For NF- κ B blocking experiments, HAECs were pretreated with 10 μ M NF- κ B inhibitor BAY 11-7082 for 1 h before exposure to M(con) or M(Hb) supernatants for 16 h. For mouse experiments, peritoneal macrophages were extracted and plated as previously described (2). Cells were exposed to Hb (0.1mg/ml) or control media 4 hours after plating and supernatant collected 12 hours later. Human and mouse VEGF-A ELISA kits were used to analyze cell culture supernatants for 7-day differentiated human macrophages from the described experiments (R&D Systems, Minneapolis, MN). Cell number was normalized to 250,000 cells/ELISA well for human macrophage experiments or 1.0×10^6 cells/well for mouse macrophage ELISA. Intracellular iron concentration was measured via colorimetric assay (Sigma).

PHD2 activity assay. The PHD2 activity assay was carried out as per the methods of Nandal et al. (3). Briefly, biotinylated peptides (Genscript) for this assay were derived from the HIF1 α oxygen-dependent degradation domain. 10ng of the biotinylated Hif1 α peptide (i.e. Biotin-Ahc- DLDLEALAPYIPADDDFQL (amino acids 556-574)) were immobilized on to 96-well Neutravidin High Binding capacity plates (Pierce cat# 15508). Plates were initially blocked with 1% BSA in TBST (25mM Tris pH7.2, 150mM NaCl and 0.05% Tween 20) for 1 hour, followed by peptide binding for 2 hrs. Cells were harvested in cold PBS and lysed with Hypotonic buffer consisting of 20mM Hepes, 5mM NaF, 10 μ M Na₃VO₄, 0.1mM EDTA, 1x protease inhibitors and 2mM DTT. Lysates were placed on ice for 15-20 mins and then 0.1% NP40 was added and samples were vortexed for 10s. Protein was estimated from clarified lysates. Hydroxylase reactions were carried out using 100 μ g/well of clarified lysates mixed with reaction buffer containing 20mM Tris-Cl (pH7.5), 5 mM KCl, 1.5mM MgCl₂, 2 mM DTT, 0.5mM 2-Oxoketoglutarate, and 1mM Ascorbic acid for 45 mins at room temperature. Three Washes were performed in between steps using 0.1% BSA TBST. Peptide hydroxylation was detected using rabbit polyclonal primary antibody against hydroxylated HIF1 α which specifically recognizes the HIF1 α hydroxylation at Proline 564 (Novus NB110-74679) for one hour and anti rabbit HRP-conjugated secondary detection antibody (Pierce SA1-9510). Ultra TMB (Pierce) and stop solution was used for color development. Chemiluminescence was detected using a microplate reader at 450nm. Each experiment was calibrated to an internal standard curve using the hydroxylated HIF1 α peptide (amino acids 556-574 Pro564) Biotin-Ahc-DLDLEALA-P(HyP)YIPADDDFQL. The assay detection allowed the detection of the hydroxylated substrate in a concentration range of 1 to 40nM. PHD activity was given as the amount of HIF1 α peptide

that was hydroxylated by 1 µg protein of the respective cell extract and expressed relative percent as compared to control lysates (4).

Endothelial permeability assays. Transendothelial electrical resistance: Human aortic endothelial cells (HAECs, Cell Applications, San Diego, CA) were seeded at 5.0×10^4 cells/cm² on a pre-constructed 8-well gelatin-coated gold electrode (Applied Biophysics, Troy, NJ) and grown to confluence. The small electrode and the larger counter-electrode were connected to a phase-sensitive lock-in amplifier. A constant current of 1 µA was supplied by a 1-V, 4000-Hz AC signal connected serially to a 1-MΩ resistor between the small electrode and larger counter-electrode. The voltage was monitored by a lock-in amplifier, stored, and processed by a personal computer. The same computer controlled the amplifier output and switched the measurement to different electrodes in the course of an experiment. Before each experiment, endothelial monolayers were washed with endothelial growth medium and used for measuring changes in TEER. TEER was measured in real-time using ECIS software (Applied Biophysics, Troy, NJ) and is expressed as specific electrical resistance (Ω cm²). Data are presented as the change in resistive portions of the resistance normalized to its value at baseline for each treatment groups and statistical comparison was made between treatment groups to exclude variation in baseline monolayer characteristics (n = 4 wells for each treatment group) as per our previous work(5).

FITC-Dextran Permeability Assay: The assay was performed as per the methods of Monaghan-Benson(6). HAECs were cultured at a concentration of $1-2 \times 10^5$ per well in 24-well on Costar®-Transwell® cell culture inserts (cat #3470). The cells were maintained in culture with 100 µl of complete media in the luminal (upper) chamber and 600 µl in the abluminal (lower) chamber. Two days later the media in both chambers were replaced with 1:1 ratio of 7 day

differentiated macrophage supernatants of control and HH human differentiated macrophages and complete growth media. The same method was used for mouse dermal microvascular endothelial cells (MDECs, Cell Biologics, Chicago, IL) and treated with supernatants from control and Hb treated WT and CD163 knock out mice peritoneal macrophages. After overnight treatment, the media in the upper chamber was replaced with fresh basal media minus phenol red containing 500ug/ml of FITC-dextran (dextran, fluorescein, 70,000 MW, FD70S Sigma) and the lower well media was replaced with basal media minus phenol red. A sample of the media in the lower wells was taken at 30 mins and transferred to a clear bottom 96-well plate (Costar #3603). The fluorescence intensity was measured using a fluorescence plate reader with filters for 485nm and 535nm wavelength excitation and emission, respectively. Data are presented as the percent change of FITC-Dextran content compared with control (n = 4 wells for each experiment).

Endothelial cell siRNA transfection. For HAEC transfections, HAEC cell monolayers were transfected with scramble (Life Technologies) and human VEGFR2 siRNA (Stealth siRNA Life technologies) in Basal media and Hiperfect transfection reagent (Qiagen). The sequence of the VEGFR2 siRNA was Sense: CCA UGU UCU UCU GGC UAC UUC UUG U Antisense: ACA AGA AGU AGC CAG AAG AAC AUG G. Transfection complexes were removed after 5 hrs and replaced with fresh media overnight. The following day the media in both chambers was replaced with 1:1 ratio of 7 day macrophage supernatants of control and HH seven day differentiated human macrophages or supernatants from 24 hour differentiated control or Hb exposed WT or *CD163*^{-/-} mouse peritoneal macrophages in combination with endothelial cell growth media. Knockdown was validated by western blotting and showed approximately 70% knockdown as compared to scramble transfected cells.

Western blotting. Protein isolated from human carotid arteries samples, processed, quantitated by BCA assay (Pierce), and separated on polyacrylamide gel as previously described (7). For detection of HIF1 α -OH, nuclear extracts from 7 day differentiated macrophages were prepared using cytoplasmic extraction Buffer A (consisting of 10mM Hepes, 10 mM KCl, 2mM MgCl₂, 0.1 mM EDTA, 0.1 mM NaF, 0.2 mM NaVO₄, 1 mM DTT, and 1x protease inhibitors) and nuclear extraction buffer B consisting of 50mM Hepes, 50mM KCl, 2mM MgCl₂, 0.1 mM EDTA, 0.1 mM NaF, 0.2 mM NaVO₄, 1 mM DTT, 300mM NaCl, 20% glycerol and protease inhibitors (Roche). Differentiated macrophages were treated with 10 μ M MG132 for 2 to 3 hours prior to harvest in cold PBS. Nuclear extracts were analyzed by western blotting and membranes probed with antibodies against rabbit HIF-OH antibody (Novus NB110-74679), and Histone 3 (Cell Signaling #4499) was used for normalization. Whole cell lysates of *in vitro* macrophage experiments were used for other western blotting experiments. Cells were lysed with 25mM Tris, 40mM KCl, 1% NP40, 1mM DTT and 1x Protease Inhibitors (Roche). Membranes were probed with indicated primary antibodies, followed by detection using horseradish peroxidase conjugated secondary antibodies (Cell Signaling) and enhanced chemiluminescence substrates (Pierce). Antibodies used were anti PHD2 (Novus NB100-2219) and mouse anti HIF1 α (BD Transduction 610958) or mouse anti-GAPDH (Novus, NB300-328) for normalization. For immunoblotting of human atherosclerotic plaque specimens, antibodies against HIF1 α (Novus NB100-134), VEGF-A (Calbiochem PC37), CD163 (Bioss bs2527R), VCAM (Abcam ab134047), phospho-NF- κ B p65 (Cell Signaling #3039), Total NF- κ B p65 (Cell Signaling #4764) and GAPDH (Novus NB300-328) were used.

Membrane fraction isolation for VE-cadherin. HAEC (Cell Applications, San Diego, CA) (P5) were transfected as described above, with scrambled (Proprietary sequence Life Technologies) and Stealth VEGFR2 siRNA (Life Technologies) using transfecting reagents HiPerfect (Qiagen) and basal media. Next day the cells were treated overnight, with a mixture of control and HH 7 day differentiated human macrophage supernatants in a 1:1 ratio with complete HAEC growth media. Cells were then scraped off the dish with cold PBS. Membrane extracts were prepared using the Qproteome subcellular fractionation kit (Qiagen). The membrane extracts were analyzed by western blotting and were probed with Rabbit VE-Cadherin (Abcam, ab33168) and mouse Na⁺K⁺ATPase (DSHB, University of Iowa) was used for normalization

Matrigel angiogenesis assay. A total of 4×10^4 HAEC resuspended in 100 μ l conditioned media were seeded in each well. (Macrophage lysates were generated as stated above). The 96-well plates were pre-coated with 50 μ l growth factor reduced-matrigel (BD Bioscience, #356234). The HAEC cells were then incubated at 37 °C for 6 h to allow the formation of tube-like structures. Images of the tubes formed were captured under inverted microscopy at $\times 10$ magnification, and the total tube length formed by each sample was measured by NIS-elements v3.0 (Nikon). Four independent experiments were performed for each sample.

Mice. The Institutional Animal Care and Use Committee at Emory University and the MedStar Health Research Institute approved all animal protocols. All animal experiments were conducted according to the National Institutes of Health Guide for the Care and Use of Laboratory Animals. CD163 knockout mice (CD163^{tm1(KOMP)Vlbg}) were generated using targeting constructs available from the University of California at Davis International Mouse Consortium (KOMP) as

previously described(8). Mice with genetic deficiency of *Apolipoprotein E* (on a *C57BL6*) were purchased from Jackson Labs and mated to *CD163*^{-/-} mice until homozygosity was achieved for both genes (i.e. *ApoE*^{-/-} *CD163*^{-/-}). These mice were compared to littermate control *ApoE*^{-/-} *CD163*^{+/+} mice. Male mice were used for all experiments. For long-term one year study, mice were maintained on regular chow diet, until one year old. Freshly collected blood samples were tested for glucose and CBC at IDEXX BioResearch (North Grafton, MA). Insulin levels were measured by using a mouse insulin ELISA kit (80-INSMS-E01, ALPCO, Salem, NH). FITC-dextran (Sigma) (50 µg/g body weight) was administered via i.v. injection, and mice were sacrificed 2 h later and perfusion fixed using formalin. Heart and aorta were harvested and embedded in O.C.T. for frozen sectioning, histology and immunofluorescence analysis. For anti-VEGF antibody treatment study, mice were administered via i.p. a rabbit anti-mouse VEGF-specific neutralizing antibody (BD0801). A rabbit IgG isotype (Cat. No. 10500C, Life Technologies) was used as a control at the dose of 2.5 mg/kg was administered twice a week for 4 weeks. At the end of the treatment, mice were given gold nanoparticle labeled monocytes 1×10⁶ cells/mouse via i.v. injection, as previously described (9). Briefly, CD11b⁺ monocytes were isolated from spleens harvested from wild-type mice using CD11b positive selection MicroBeads (Miltenyi) following manufacturer's instruction, and cultured in 6-well plate. Cells were incubated with 0.5 mg Au/mL gold nanoparticles for 24 h for labeling, before washing and injection. The aortas were harvested 7 days from mice after i.v. injection.

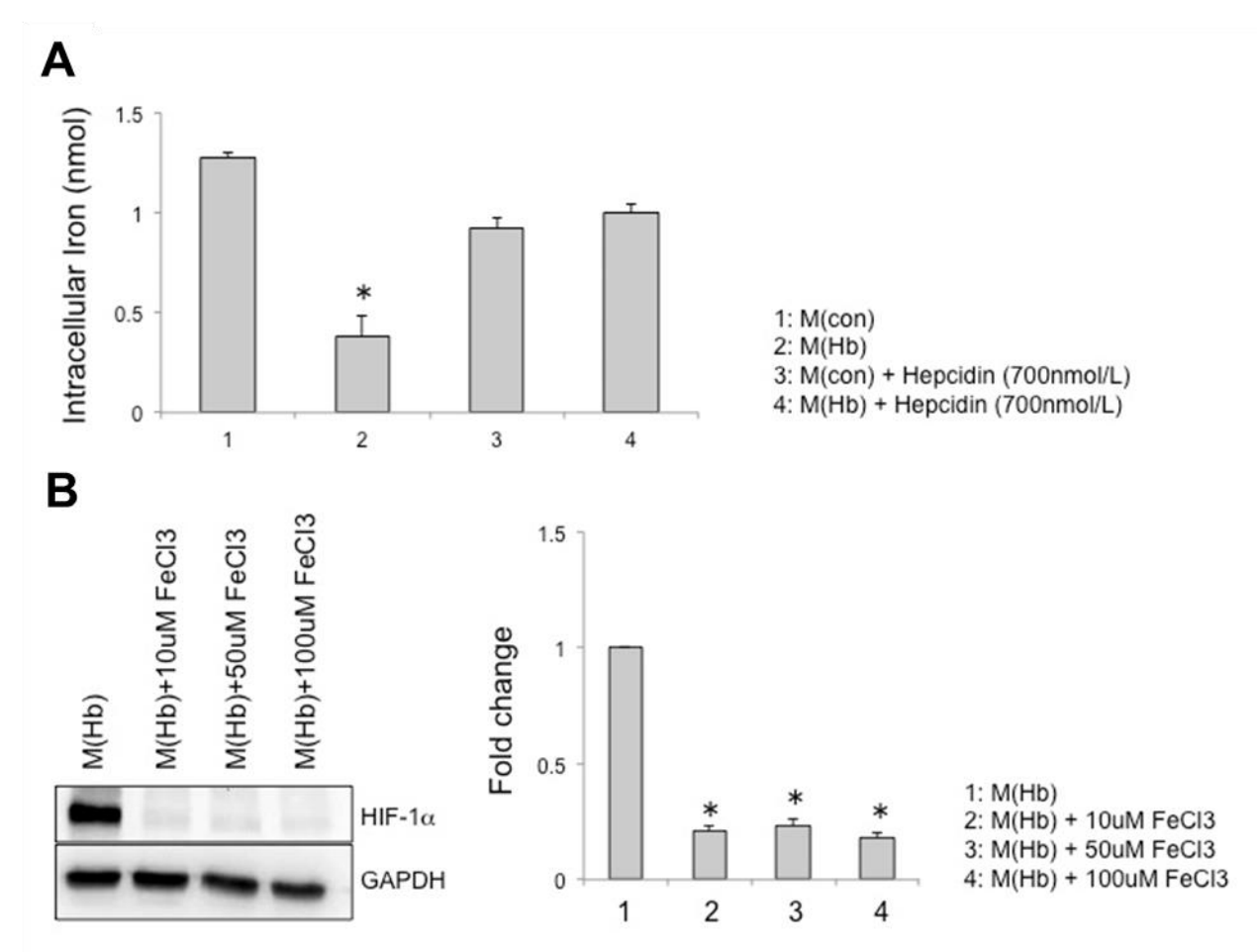
Mouse histology and immunofluorescent staining. Tissue samples were embedded in Optimal Cutting Temperature (O.C.T.) compound and frozen, followed by sectioning at 10 µm thickness. Slides were stained by H&E and Movat Pentachrome for histological analysis. For

immunofluorescence, sections were incubated in primary antibodies TER119 at a dilution of 1:100 (cat. #: 116201 from BioLegend), Mac-3 at a dilution of 1:100 (Cat #: 101447 from Santa Cruz), VE-cadherin at a dilution of 1:250 (cat #:ab33168, Abcam), VCAM at a dilution of 1:100 (Cat #: ab134047, Abcam), CD163 antibody at a dilution of dilution 1:250 (clone number TNKUPJ from eBiosciences) for 16 h at 4 °C. Alexa Fluor labeled secondary antibodies (Life Technologies) were used for further incubation. Proper positive and negative controls were included in every immunostaining. Tissue samples were mounted on slides with Vectashield mounting medium (Vector Labs, Burlingame, CA). Tissue was visualized using objective on a LSM 700, 800, or 880 laser scanning confocal microscopy (Zeiss). Projection images were generated by collecting the maximum pixel intensity from each image of the Z stack and by projecting pixel intensity onto the single (projection) image. Staining area was quantified using computer-aided planimetry and was expressed as a percentage of the total surface area of the tissue section.

Statistics. Analysis of normality of continuous variables was performed using a Shapiro-Wilk test. Normally and non-normally distributed data were analyzed for significance by student's *t*-test or Mann-Whitney-Wilcoxon tests, respectively. For quantification of *in vitro* studies presented, a minimum of 4 replicates were tested for each condition of experiment. The data are represented as mean \pm SEM or SD (as indicated). For multiple group comparisons, we utilized a one-way ANOVA. If the variance ratio test (F-test) was significant, a more detailed post hoc analysis of differences between groups was made using a Tukey-Kramer honest significance difference test. In the SNP analysis of CVPPath Cohort, Fisher's exact test was used to compare the two genotypes. In the SNP analysis of ARIC cohort described above, Cox proportional

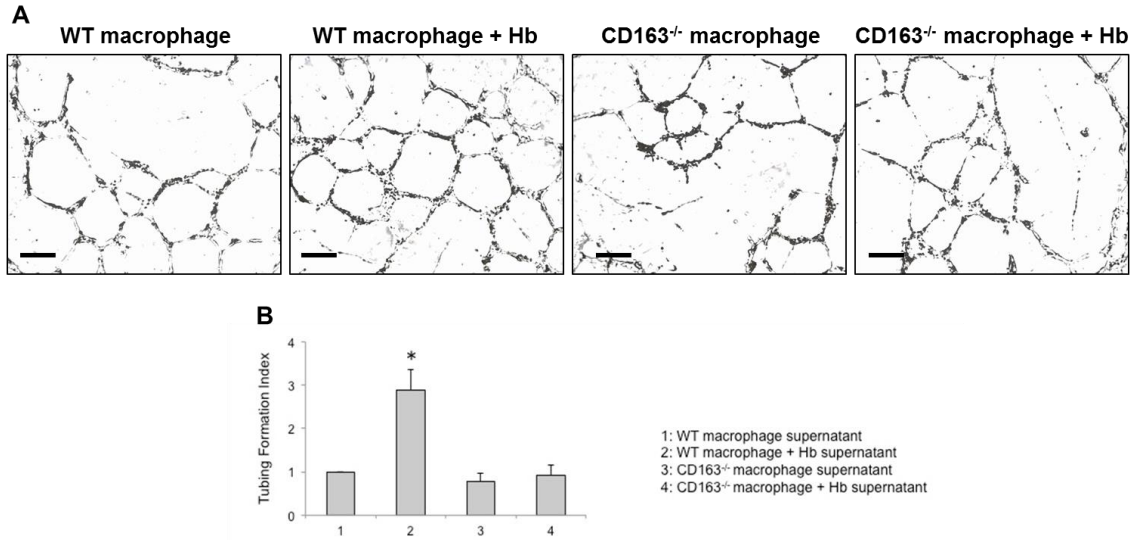
hazards models were used to examine the association of genetic variant with incident MI and incident CHD, and the analyses were adjusted for age, sex, ancestry-informative principal components, and study center. A p value <0.05 was considered statistically significant.

Supplemental Figures:



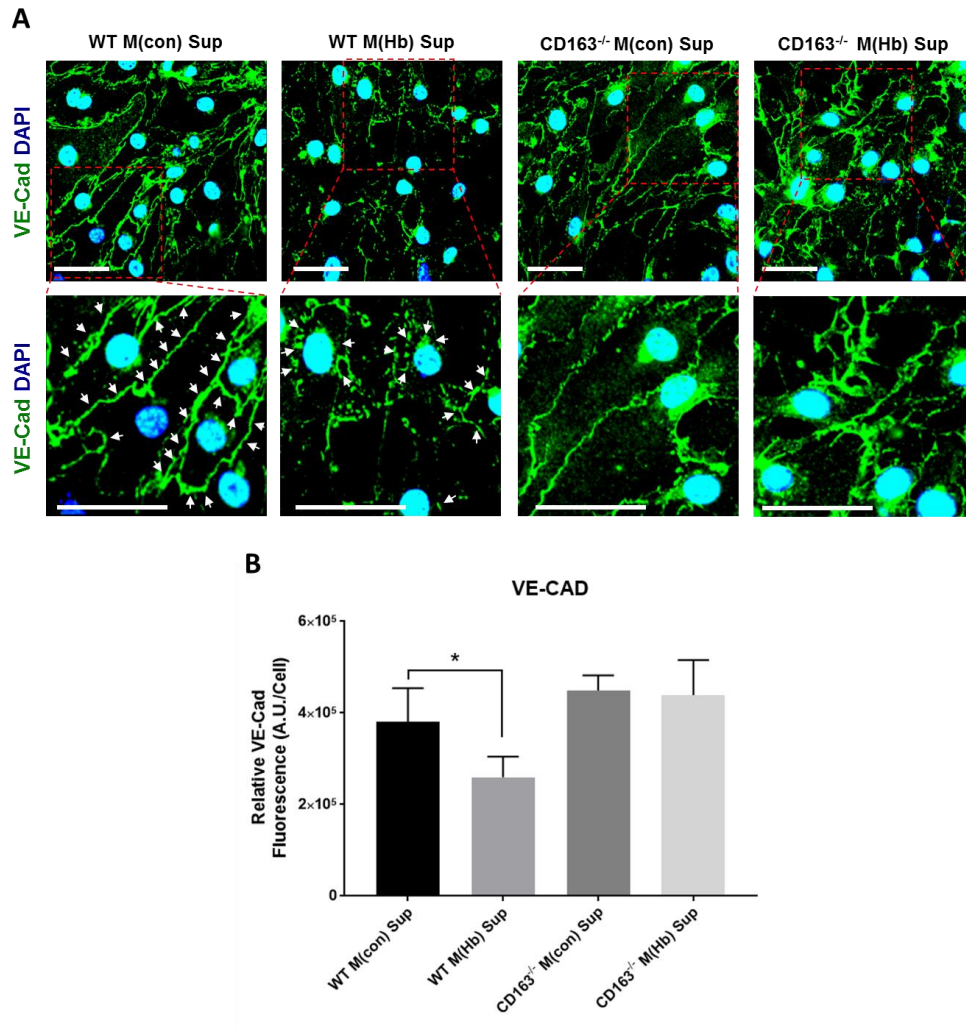
Supplemental Figure 1. Within M(Hb) activation of HIF-1 α is dependent upon intracellular Iron.

A, Intracellular iron levels in control (M(con)) or hemoglobin:haptoglobin differentiated (M(Hb)) human macrophages treated with or without Hepcidin (700nmol/L) 24 hours before analysis. (n=4 per each group) **B**, Immunoblotting of human macrophages (n=4 per group) with quantitation of densitometry for HIF-1 α . For multiple group comparisons, we utilized a one-way ANOVA. If the variance ratio test (F-test) was significant, a more detailed post hoc analysis of differences between groups was made using a Tukey-Kramer honest significance difference test. All bars show mean \pm SEM. *, $p < 0.05$ versus other groups in **A**, versus M(Hb) in **B**.



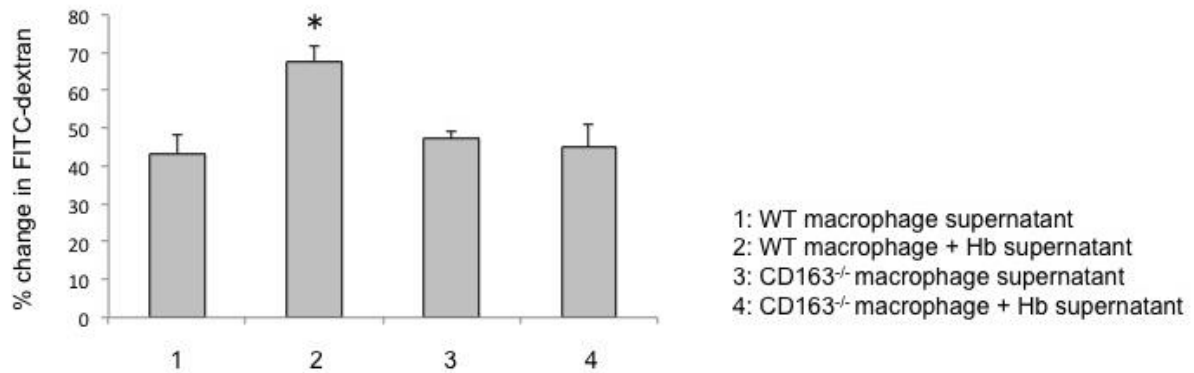
Supplemental Figure 2. Hb ingestion by macrophages induces angiogenesis via CD163.

Tube formation assays of mouse dermal endothelial cell (MDEC) treated with mouse macrophages supernatants (1: WT macrophages, 2: Hb stimulated WT macrophages, 3: CD163^{-/-} macrophages, 4: Hb stimulated CD163^{-/-} macrophages). **A.** Relative tube-forming abilities were determined and representative images are shown on the top. Scale bar indicates 200 μ m. **B.** Tubing formation index shown as fold change relative to group 1. For multiple group comparisons, we utilized a one-way ANOVA. If the variance ratio test (F-test) was significant, a more detailed post hoc analysis of differences between groups was made using a Tukey-Kramer honest significance difference test. All bars show mean \pm SEM. *, $p < 0.05$ versus other groups.



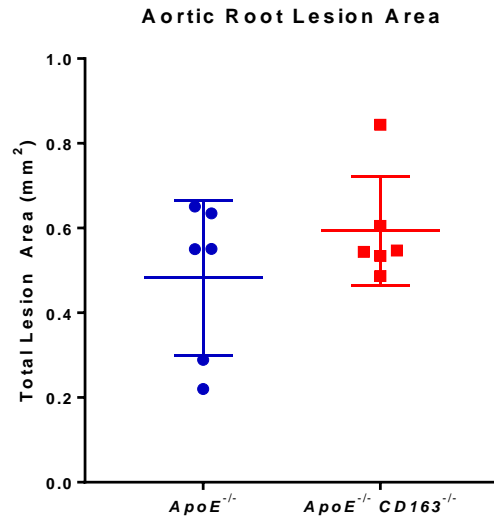
Supplemental Figure 3. Hb ingestion by macrophages promotes VE-cadherin internalization and degradation via CD163.

A. First row shows immunofluorescent imaging of mouse dermal endothelial cell (MDEC) and treated with mouse macrophage supernatants as described for VE cadherin (green) and DAPI (blue) is shown ($\times 60$). Row 2 shows high power images in red boxed regions above. White scale bar indicates 50 μm . MDECs treated with mouse macrophage supernatants (1: WT macrophages, 2: Hb stimulated WT macrophages, 3: CD163^{-/-} macrophages, 4: Hb stimulated CD163^{-/-} macrophages). Arrows indicate the difference of VE-cadherin located in plasma membrane in 1. and internalization and degradation in 2. **B.** Quantitation of plasma membrane VE-cadherin in experiment shown. (n=4-5 per group). For multiple group comparisons, we utilized a one-way ANOVA. If the variance ratio test (F-test) was significant, a more detailed post hoc analysis of differences between groups was made using a Tukey-Kramer honest significance difference test. All bars show mean \pm SEM. *, $p < 0.05$ versus other groups.

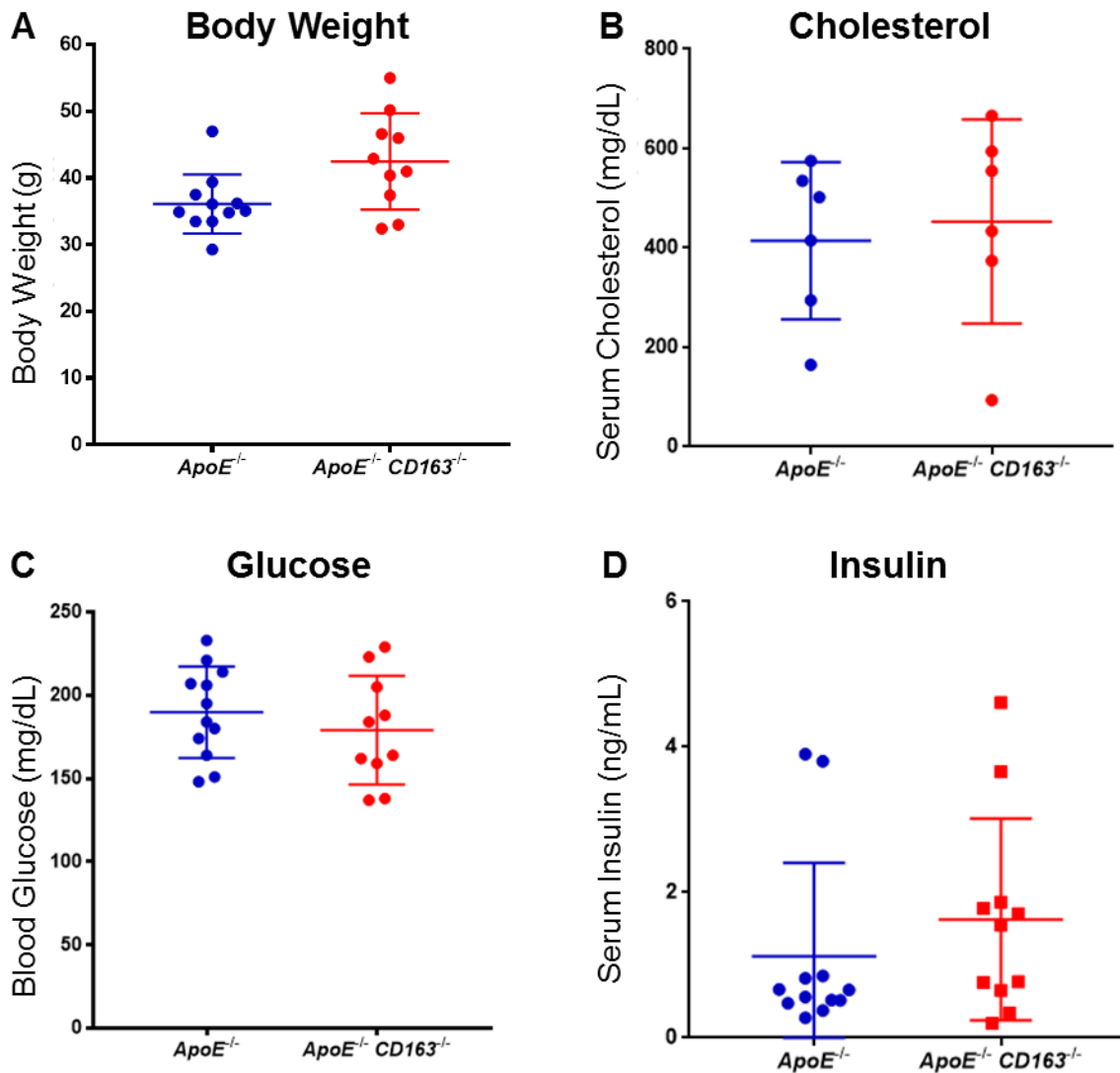


Supplemental Figure 4. Hb ingestion by macrophages promotes vascular permeability via CD163.

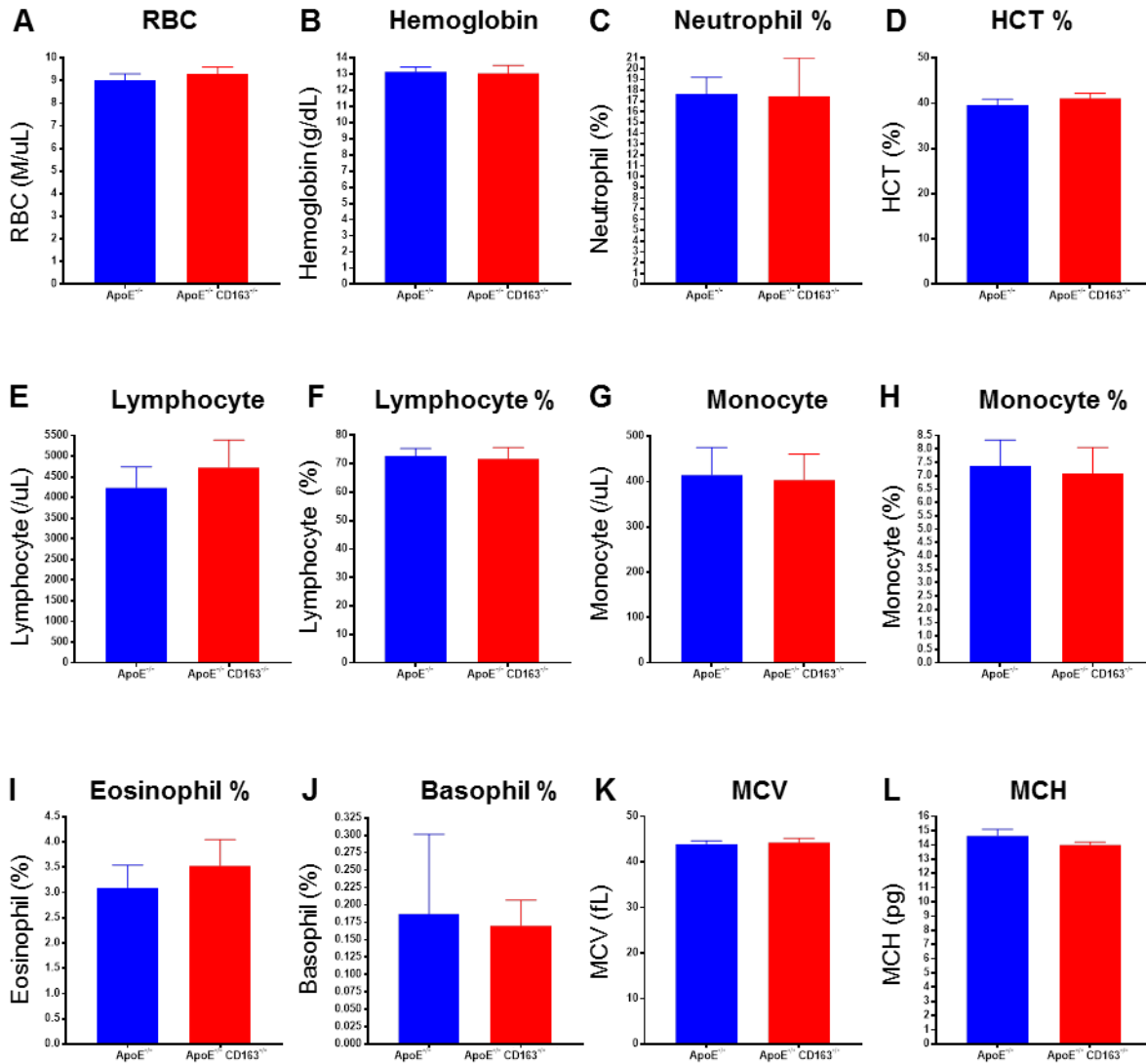
FITC-Dextran permeability of MDECs treated with mouse macrophage supernatants (1: WT macrophages, 2: Hb stimulated WT macrophages, 3: CD163^{-/-} macrophages, 4: Hb stimulated CD163^{-/-} macrophages). Percent change of FITC-dextran compared with control (WT) supernatant is shown. For multiple group comparisons, we utilized a one-way ANOVA. If the variance ratio test (F-test) was significant, a more detailed post hoc analysis of differences between groups was made using a Tukey-Kramer honest significance difference test. All bars show mean ± SEM. *, $p < 0.05$ versus other groups.



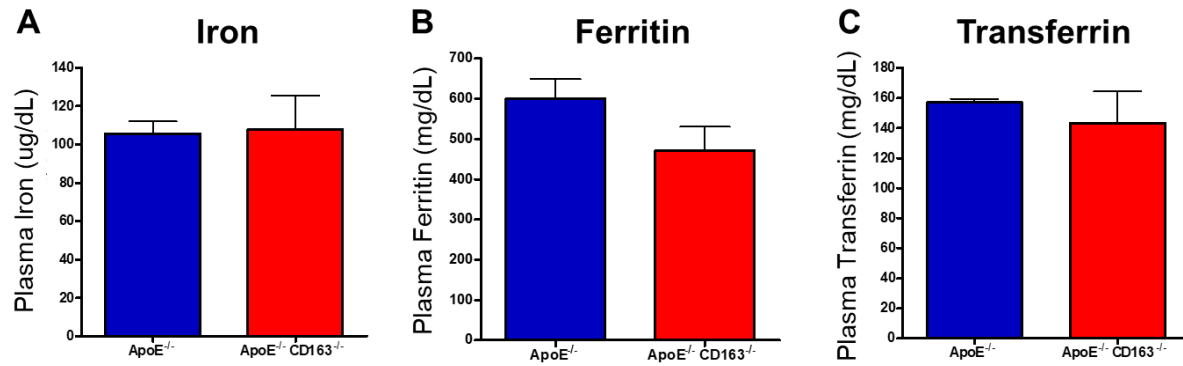
Supplemental Figure 5. Aortic root total lesion area quantification in one-year-old *ApoE*^{-/-} and *ApoE*^{-/-} *CD163*^{-/-} mice. The Plot shows mean \pm SD. Comparisons between two groups were achieved using a two-sided student's *t*-test. Result showed no statistically significant difference. (n=6 per group).



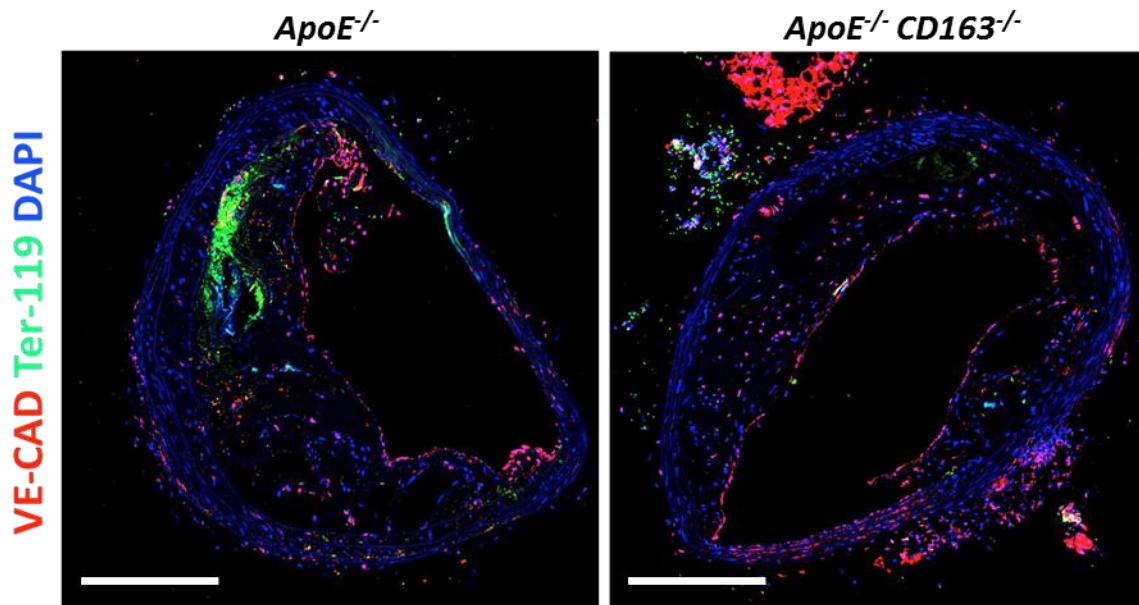
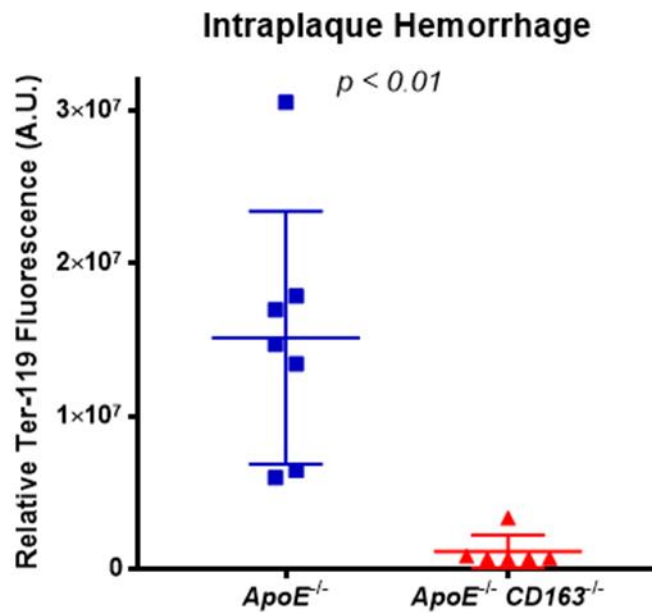
Supplemental Figure 6. Body weight, serum cholesterol, blood glucose, and insulin concentrations in one-year-old *ApoE*^{-/-} and *ApoE*^{-/-} *CD163*^{-/-} mice. A. Body weight. B. Serum Cholesterol. C. Blood glucose concentrations. D. Insulin concentrations. (n=6-12 per group). All plots show means \pm SD. Comparisons between two groups were achieved using a two-sided student's *t*-test. All results showed no statistically significant difference.



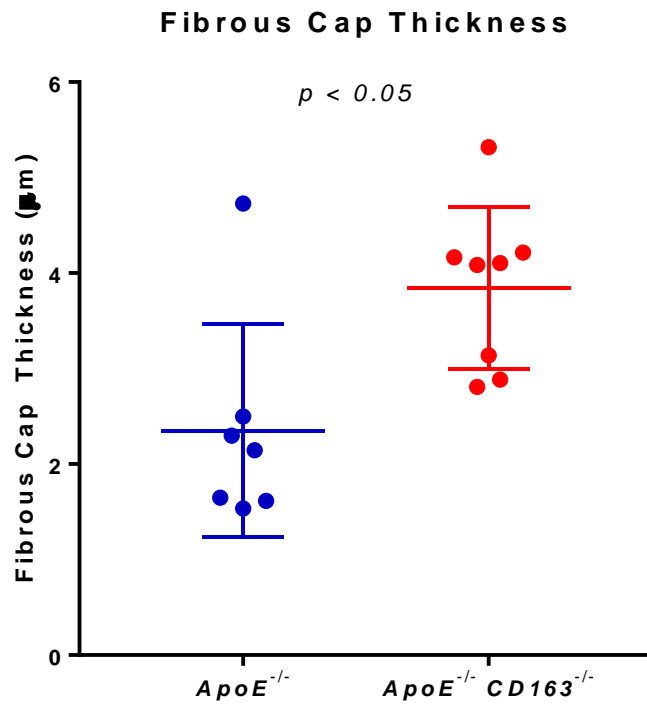
Supplemental Figure 7. Complete blood counts and white blood cells differential in one-year-old *ApoE*^{-/-} and *ApoE*^{-/-} *CD163*^{-/-} mice. A. Red blood cells (RBC). B. Hemoglobin. C. Neutrophil. D. Hematocrit (HCT). E. Lymphocyte. F. Lymphocyte %. G. Monocyte. H. Monocyte %. I. Eosinophil. J. Basophil. K. Mean Corpuscular Volume (MCV). L. Mean Corpuscular Hemoglobin (MCH). Other cell types, including metamyelocyte, myelocyte, promyelocyte, were not seen. (n=10-12 per group). All bars show means ± SEM. Comparisons between two groups were achieved using a two-sided student's *t*-test. All results showed no statistically significant difference.



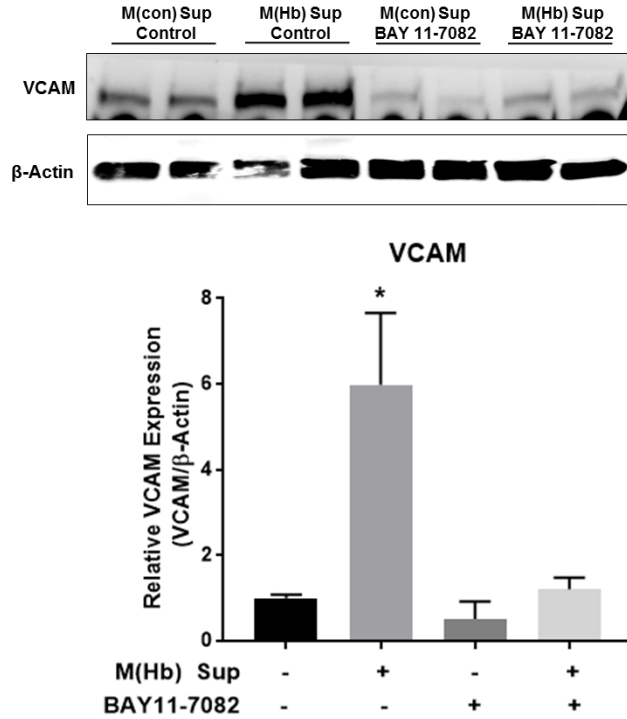
Supplemental Figure 8. Plasma iron, ferritin, and transferrin concentrations in one-year-old *ApoE*^{-/-} and *ApoE*^{-/-} *CD163*^{-/-} mice. **A.** Plasma iron concentrations. **B.** Plasma ferritin concentrations. **C.** Plasma transferrin concentrations. (n=5-6 per group). All bars show means \pm SEM. Comparisons between two groups were achieved using a two-sided student's *t*-test. All results showed no statistically significant difference.

A**B**

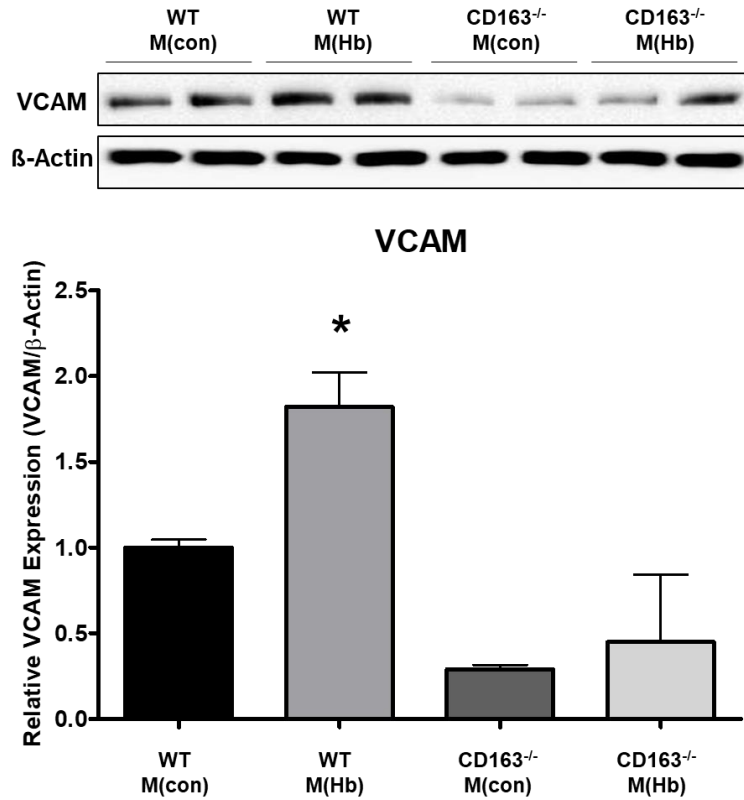
Supplemental Figure 9. Intraplaque hemorrhage assessment by immunostaining. A. immunofluorescence images of VE-CAD (red) and Ter-119 (green) in BCA plaques from one-year-old *ApoE*^{-/-} and *ApoE*^{-/-} *CD163*^{-/-} mice. Scale bar is 100 μ m. **B.** Quantitation of Ter-119 immunofluorescence. (n=6-7 per group). The Plot shows mean \pm SD. Comparisons between two groups were achieved using a two-sided student's *t*-test.



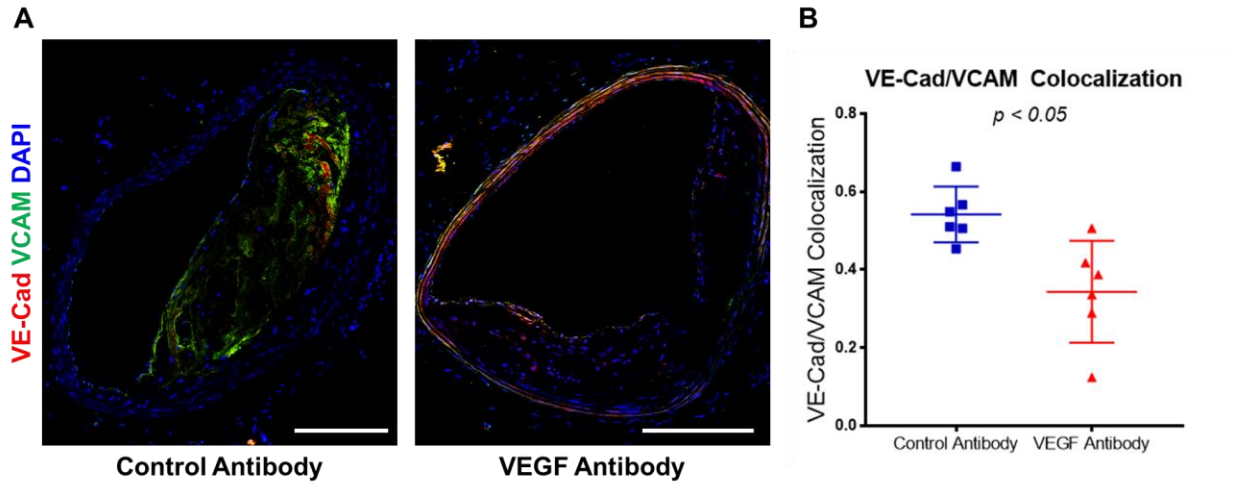
Supplemental Figure 10. Fibrous cap thickness in BCA plaque is higher in one-year-old $ApoE^{-/-} CD163^{-/-}$ versus $ApoE^{-/-}$ controls. (n=7-8 per group). The Plot shows mean \pm SD. Comparisons between two groups were achieved using a two-sided student's *t*-test.



Supplemental Figure 11. Activation of VCAM in Human Aortic Endothelial Cells (HAECs) is blocked by NF- κ B inhibitor. Human aortic endothelial cells were pretreated with 10 μ M NF- κ B inhibitor BAY 11-7082 for 1 h before exposure to M(con) or M(Hb) supernatants for 16 hours. The expression of VCAM was measured by immunoblotting. $n=4$ per group. For multiple group comparisons, we utilized a one-way ANOVA. If the variance ratio test (F-test) was significant, a more detailed post hoc analysis of differences between groups was made using a Tukey-Kramer honest significance difference test. All bars show mean \pm SEM. *, $p<0.05$ versus all other groups.



Supplemental Figure 12. Immunoblotting of mouse dermal endothelial cell (MDEC) treated with mouse macrophage supernatants (1: WT macrophages, 2: Hb stimulated WT macrophages, 3: CD163^{-/-} macrophages, 4: Hb stimulated CD163^{-/-} macrophages). n=4 per group. For multiple group comparisons, we utilized a one-way ANOVA. If the variance ratio test (F-test) was significant, a more detailed post hoc analysis of differences between groups was made using a Tukey-Kramer honest significance difference test. All bars show mean \pm SEM. *, $p < 0.05$ versus all other groups.



Supplemental Figure 13. Immunofluorescence of VE-cadherin (red) and VCAM(green) in BCA plaques from 6-8 month old *ApoE*^{-/-} mice treated with control or anti-VEGF antibodies. **A. Representative images of VE-cadherin and VCAM staining. **B.** Quantification of VE-cadherin and VCAM colocalization. Scale bar is 100 μ m. (n=6 per group). The Plot shows mean \pm SD. Comparisons between two groups were achieved using a two-sided student's *t*-test.**

Supplemental Tables

Supplemental Table 1. Demographic data and risk factors between subjects of different genotypes in rs7136716 in the CVPath Registry.

rs7136716	AA (111)	AG (175)	GG (60)	p-value
Age (yrs)	48.0±10.1	47.3±10.8	49.6±14.2	0.391
Male [n(%)]	77 (69.4%)	128 (73.1%)	41 (68.3%)	0.690
BMI (kg/m ²)	31.8±8.8	31.1±8.9	30.5±7.1	0.618
Hypertension [n(%)]	46 (41.4%)	70 (40%)	28 (33%)	0.664
Hyperlipidemia [n(%)]	12 (10.8%)	16 (9.1%)	1 (6%)	0.105
Diabetes [n(%)]	22 (19.8%)	20 (11.4%)	7 (17%)	0.116
Smoking [n(%)]	6 (5.4%)	11 (6.3%)	9 (15%)	0.052

Supplemental Table 2. Demographic data and risk factors between subjects of homozygous major A allele and homozygous minor G allele in rs7136716 in ruptured plaques from the CVPath registry.

rs7136716	AA (22)	GG (25)	p-value
Age (yrs)	48.0±7.2	54.0±14.1	0.079
Male [n(%)]	20 (90.1%)	22 (88.0%)	1.000
BMI (kg/m ²)	30.7±5.7	30.7±5.4	0.999
Hypertension [n(%)]	7 (31.8%)	9 (36.0%)	0.755
Hyperlipidemia [n(%)]	1 (4.5%)	1 (4.0%)	1.000
Diabetes [n(%)]	4 (18.2%)	4 (16.0%)	1.000
Smoking [n(%)]	1 (4.5%)	3 (12.0%)	0.612

Supplemental Table 3. Baseline Demographic characteristics of the 3225 included participants from the Atherosclerosis Risk in Communities Study.

Demographic Characteristics	Mean (SD) or N (%)
Age (yrs)	53.55 (5.84)
Male [n(%)]	1201 (37)
Hypertension[n(%)]	1795 (56)
Diabetes[n(%)]	629 (20)
Current smoker[n(%)]	985 (31)
Total cholesterol (mg/dL)	214.83 (45.20)
Triglyceride (mg/dL)	135.65 (90.91)
BMI (kg/m ²)	29.69 (6.28)

Supplemental Table 4. The inflammation scoring matrix. Plaque inflammation was semi-quantitatively assessed using a scoring system accounting for both the severity by the number of inflammatory cells and relative distribution based on quadrants. Severity was scored 0 to 4: 0-20 inflammatory cells = 0, 21-100 cells= 1, 101-200 cells = 2, 201-400 = 3, >400 cells = 4. Distribution was also scored 0 to 4, 0-45 degrees = 0, 45-90 degrees = 1, 90-180 degrees = 2, 180-270 degrees = 3, 270- 360 degrees = 4. The overall inflammation score was drawn from the scoring matrix below.

		Distribution (Degrees)				
		0-45	45-90	90-180	180-270	270-360
Severity (Cells)	0-20	0	1	2	3	4
	21-100	1	2	3	4	5
	101-200	2	3	4	5	6
	201-400	3	4	5	6	7
	>400	4	5	6	7	8

Supplemental Table 5. Demographic characteristics and risk factors of subjects selected for coronary artery Evans Blue perfusion study.

Demographic Characteristics	Mean \pm SD or N (%)
Age (years)	39.6 \pm 9.1
Male [n(%)]	5 (100%)
Hypertension [n(%)]	2 (40%)
Hyperlipidemia [n(%)]	1 (20%)
Diabetes [n(%)]	1 (20%)
Smoking [n(%)]	2 (40%)
BMI (kg/m ²)	31.4 \pm 3.4

References

1. Finn, A.V., Nakano, M., Polavarapu, R., Karmali, V., Saeed, O., Zhao, X., Yazdani, S., Otsuka, F., Davis, T., Habib, A., et al. 2012. Hemoglobin directs macrophage differentiation and prevents foam cell formation in human atherosclerotic plaques. *J Am Coll Cardiol* 59:166-177.
2. Saeed, O., Otsuka, F., Polavarapu, R., Karmali, V., Weiss, D., Davis, T., Rostad, B., Pachura, K., Adams, L., Elliott, J., et al. 2012. Pharmacological suppression of hepcidin increases macrophage cholesterol efflux and reduces foam cell formation and atherosclerosis. *Arterioscler Thromb Vasc Biol* 32:299-307.
3. Nandal, A., Ruiz, J.C., Subramanian, P., Ghimire-Rijal, S., Sinnamon, R.A., Stemmler, T.L., Bruick, R.K., and Philpott, C.C. 2011. Activation of the HIF prolyl hydroxylase by the iron chaperones PCBP1 and PCBP2. *Cell Metab* 14:647-657.
4. Berchner-Pfannschmidt, U., Tug, S., Trinidad, B., Oehme, F., Yamac, H., Wotzlaw, C., Flamme, I., and Fandrey, J. 2008. Nuclear oxygen sensing: induction of endogenous prolyl-hydroxylase 2 activity by hypoxia and nitric oxide. *J Biol Chem* 283:31745-31753.
5. Habib, A., Karmali, V., Polavarapu, R., Akahori, H., Cheng, Q., Pachura, K., Kolodgie, F.D., and Finn, A.V. 2013. Sirolimus-FKBP12.6 impairs endothelial barrier function through protein kinase C- α activation and disruption of the p120-vascular endothelial cadherin interaction. *Arterioscler Thromb Vasc Biol* 33:2425-2431.
6. Monaghan-Benson, E., and Wittchen, E.S. 2011. In vitro analyses of endothelial cell permeability. *Methods Mol Biol* 763:281-290.
7. Finn, A.V., John, M., Nakazawa, G., Polavarapu, R., Karmali, V., Xu, X., Cheng, Q., Davis, T., Raghunathan, C., Acampado, E., et al. 2009. Differential healing after sirolimus, paclitaxel, and bare metal stent placement in combination with peroxisome proliferator-activator receptor gamma agonists: requirement for mTOR/Akt2 in PPARgamma activation. *Circ Res* 105:1003-1012.
8. Akahori, H., Karmali, V., Polavarapu, R., Lyle, A.N., Weiss, D., Shin, E., Husain, A., Naqvi, N., Van Dam, R., Habib, A., et al. 2015. CD163 interacts with TWEAK to regulate tissue regeneration after ischaemic injury. *Nat Commun* 6:7792.
9. Chhour, P., Naha, P.C., O'Neill, S.M., Litt, H.I., Reilly, M.P., Ferrari, V.A., and Cormode, D.P. 2016. Labeling monocytes with gold nanoparticles to track their recruitment in atherosclerosis with computed tomography. *Biomaterials* 87:93-103.